

# Allogeneic Mesenchymal Stem Cell Therapy for Bisphosphonate-Related Jaw Osteonecrosis in Swine

Yunsheng Li,<sup>1,2,\*</sup> Junji Xu,<sup>1,\*</sup> Lisha Mao,<sup>1</sup> Yi Liu,<sup>1</sup> Runtao Gao,<sup>1</sup> Zongmei Zheng,<sup>1</sup> Wanjun Chen,<sup>3</sup> Anh Le,<sup>4</sup> Songtao Shi,<sup>4</sup> and Songlin Wang<sup>1,5</sup>

Bisphosphonates (BPs), which are used to treat a variety of clinical disorders, have the side effect of jawbone necrosis. Currently, there is no reliable treatment for BP-related osteonecrosis of the jaw (BRONJ) due to a lack of understanding of its pathogenesis. To investigate the pathogenesis of BRONJ and observe the treatment effect of bone marrow mesenchymal stem cell (BMMSC) transplantation, we established a preclinical animal model of BRONJ in miniature pigs (minipigs). After treatment with zoledronic acid, the clinical and radiographic manifestations of BRONJ could be observed in minipigs after first premolar extraction. The biological and immunological properties of BMMSCs were impaired in the BP-treated minipigs. Moreover, the ratio of Foxp3-positive regulatory T-cells (Tregs) in peripheral blood decreased, and interleukin (IL)-17 increased in the serum of BP-treated minipigs. After allogeneic BMMSC transplantation via intravenous infusion, mucosal healing and bone reconstruction were observed; IL-17 levels were reduced; and Tregs were elevated. In summary, we established a clinically relevant BRONJ model in minipigs and tested a promising allogeneic BMMSC-based therapy, which may have potential clinical applications for treating BRONJ.

## Introduction

**B**ISPHOSPHONATES (BPs) HAVE BEEN widely used to prevent skeletal-related events, reduce bone pain, and improve the quality of life. However, literatures suggest that the use of BPs may be associated with osteonecrosis of the jaw [1,2]. BP-related osteonecrosis of the jaw (BRONJ) is defined as exposed bone in the maxillofacial region that persists for more than 8 weeks in patients with current or previous BP treatment without a history of radiation therapy to the jaw [3]. Lately, many risk factors, including BP potency, duration of BP therapy, dentoalveolar surgery, inflammatory dental diseases, and increased age, have been reported related to BRONJ [4]; however, the pathogenesis of BRONJ still remains unclear [5]. Previously, we developed a mouse model of BRONJ-like disease, disclosed the immunity-based mechanism of BRONJ-like disease, and reversed it with bone marrow mesenchymal stem cells (BMMSCs) [6]. However, treatment of BRONJ in the clinical setting is still a challenging issue [7], and preclinical studies based on a well-established large-animal model are needed.

Compared with rodents, large-animal models are superior because of their similarities in gross anatomy and physiology to humans as well as spontaneous development of diseases seen in humans involving similar processes [8]. We previously generated a miniature-pig (minipig) model of advanced osteoradionecrosis and cured it with BMMSC transplantation [9]. In the present study, we established a large-animal model of BRONJ in minipigs and observed the biological and immunological properties of BMMSCs in this animal model. Further, we demonstrated that allogeneic BMMSC transplantation cured BRONJ in minipigs. Because of the close similarity between minipigs and humans in terms of histology and functions of the orofacial tissues [8], this experimental design may yield important preclinical information about the application of stem cell-based therapy for treating BRONJ in humans.

## Materials and Methods

All study procedures were reviewed and approved by the animal care and use committee of the Capital Medical

<sup>1</sup>Molecular Laboratory for Gene Therapy & Tooth Regeneration, Beijing Key Laboratory of Tooth Regeneration and Function Reconstruction, Capital Medical University School of Stomatology, Beijing, China.

<sup>2</sup>Department of Stomatology, Coal General Hospital, Beijing, China.

<sup>3</sup>Mucosal Immunology Section, National Institute of Dental and Craniofacial Research, National Institutes of Health, Bethesda, Maryland.

<sup>4</sup>Center for Craniofacial Molecular Biology, Herman Ostrow School of Dentistry, University of Southern California, Los Angeles, California.

<sup>5</sup>Department of Biochemistry and Molecular Biology, Capital Medical University School of Basic Medical Sciences, Beijing, China.

\*These two authors contributed equally to this study.

University. All the methods conformed to the Animal Research Reporting In Vivo Experiments guidelines.

### Animals and generation of a BRONJ animal model

Inbred Wuzhishan minipigs [8], aged 12 months and weighing 30 to 40 kg, were obtained from the Institute of Animal Science of the Chinese Agriculture University (Beijing, China), and eight BRONJ models were successfully setup by being intravenously injected with zoledronic acid (ZA; Zometa; 4 mg every 2 weeks) and the first premolar extraction. Three minipigs served as control. The miniature pigs were anesthetized with a combination of 6 mg/kg ketamine chloride and 0.6 mg/kg xylazine (intramuscular injection) before all experimental procedures. Computed tomography (CT, 96 DPI; GE Medical Systems HiSpeed NX/i, General Electric Company) was used in the Beijing Friendship Hospital, Capital Medical University, Beijing, China, to assist in designing of the irradiation plan and for morphological observation. Teeth were extracted in a sterile animal operating room. Animals were anesthetized, and the first premolar was extracted with dental forceps. After tooth extraction, animals were given penicillin (30,000 U/kg, intramuscular injection) to prevent infection (see Supplementary Methods for more details; Supplementary Data are available online at [www.liebertpub.com/scd](http://www.liebertpub.com/scd)).

### BMMSC isolation, cell culture, and characterization

Porcine BMMSCs were isolated from iliac crest bone aspirates. For bone marrow harvesting, animals were anesthetized, and bone marrow was harvested from iliac crest bone aspirates by a syringe. For MSC characterization, cell surface marker such as STRO-1 and CD146 cells were observed; BrdU, CCK8, and carboxyfluorescein succinimidyl ester (CFSE) were used for self-renewal capacity determination, and multilineage differentiation potentials such as adipogenic and osteogenic were also observed (see Supplementary Methods for details).

### BrdU staining, cell counting, and CFSE labeling

The proliferation of BMMSCs was detected by BrdU staining, cell counting, and CFSE labeling. BrdU was added in the medium and stained; the BrdU-positive cells were counted and expressed as a percentage of the total number of cells. For cell counting, CCK-8 (Dojindo Laboratories) was used and measured at 450 nm. CFSE (Invitrogen) was used for cell staining ( $5 \mu\text{M}/1 \times 10^6$  cells/mL) and proliferation index flow cytometric analysis (see Supplementary Methods for details).

### Determination of apoptotic cells

BMMSC apoptosis was evaluated using the Annexin-V-FLUOS apoptosis staining kit (Roche Diagnostic). A total of  $10^6$  cells were washed with phosphate-buffered saline (PBS; Invitrogen) and centrifuged at 200 g for 5 min. The cell pellet was resuspended in 100  $\mu\text{L}$  of Annexin-V-FLUOS labeling solution, incubated, and analyzed by flow cytometry.

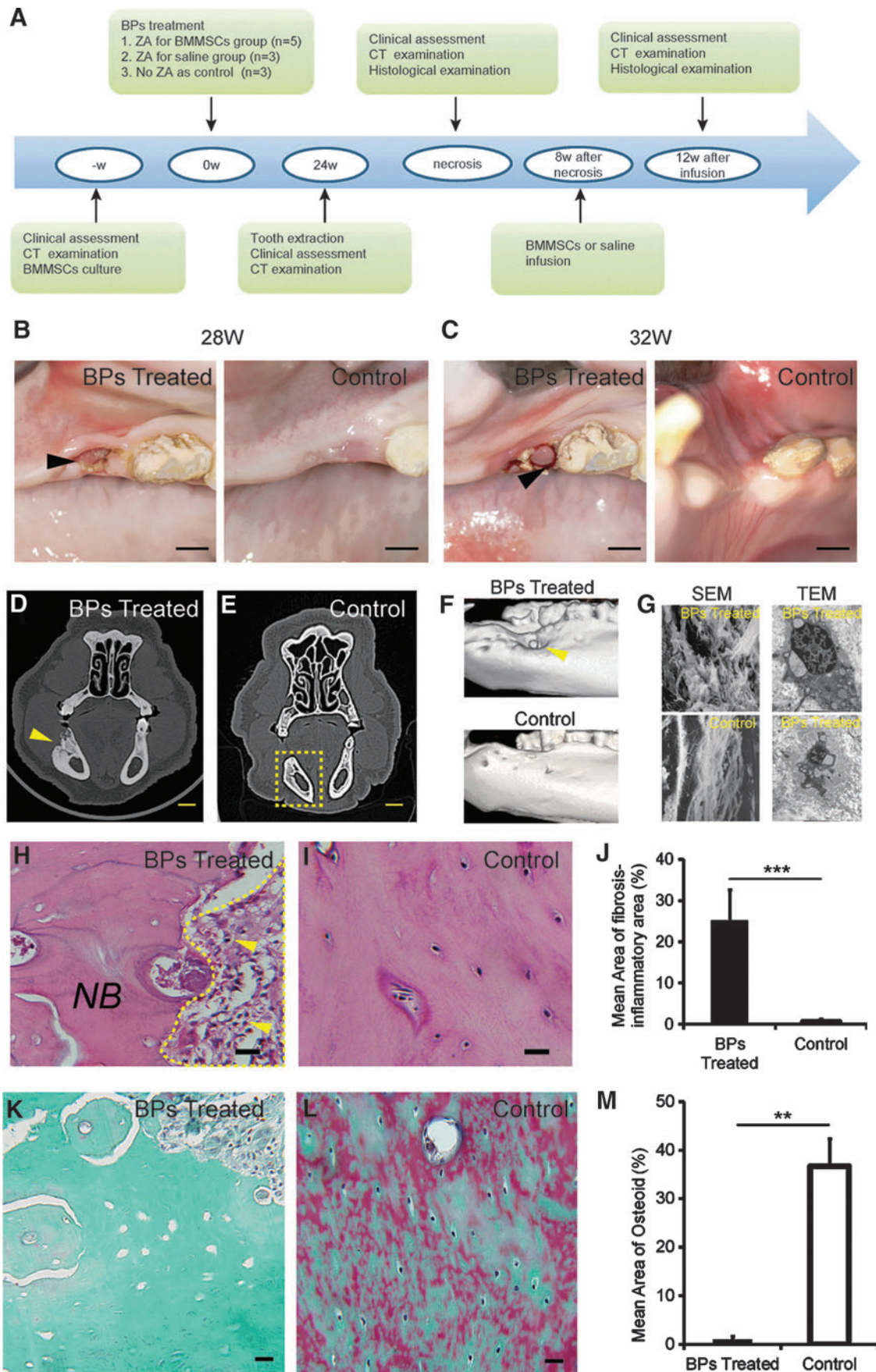
### Flow cytometry of BMMSCs

BMMSCs were harvested and incubated for 1 h with specific monoclonal antibodies against Stro-1 (R&D Systems), CD146 (Abcam), SLA-I (AbD Serotec), and SLA-II (AbD Serotec) for 1 h. After washing with PBS (Invitrogen), the cells were incubated with FITC-conjugated goat anti-mouse IgG, IgM, and IgA antibodies (AbD Serotec) for 30 min in the dark at room temperature. The antibodies were used at the concentrations suggested by the manufacturers. The cells were analyzed by fluorescein-activated cell sorter (FACS) Calibur flow cytometry.

### Immunoregulatory activity of BMMSCs

Human peripheral blood lymphocytes (hPBLs) from healthy donors were cocultured with equal numbers of BMMSCs. The proliferation of hPBLs was determined by CCK-8 (see Supplementary Methods for details).

**FIG. 1.** Generation of a minipig model of bisphosphonate (BP)-related osteonecrosis of the jaw (BRONJ). **(A)** Schematic illustration of the timeline of the procedures conducted in this study. Eight minipigs were intravenously injected with 4 mg zoledronic acid (ZA) alone once every 2 weeks. Three minipigs were injected with physiological saline as controls. Clinical assessments and computed tomography (CT) examinations were performed for all animals before BP delivery, 24 weeks before tooth extraction, after jaw bone necrosis, and 12 weeks after bone marrow mesenchymal stem cell (BMMSC) infusion. Jaw bone tissue samples were taken for histopathological analysis from all BRONJ minipigs and untreated normal controls before allogeneic BMMSC infusion and 12 weeks after the infusion. **(B)** Four weeks after extraction, the clinical examination showed incomplete mucosal healing (*black arrowhead*) in all pigs in the BP treatment group, but no pigs in the untreated group (scale bar = 1 cm). **(C)** Eight weeks after extraction, necrotic bone was exposed in the oral cavity of BP-treated minipigs (*black arrowhead*), but not in the untreated group (scale bar = 1 cm). **(D)** After tooth extraction, destruction and enlargement of the cortical bone were seen in the BRONJ model on the CT scan. Both osteolysis and osteosclerosis were observed in the necrotic jaw bone (*yellow arrowhead*) (scale bar = 1 cm). **(E)** The CT scan showed a healed alveolar socket (*yellow frame*) in the control group (scale bar = 1 cm). **(F)** The 3D images of CT scan showed destruction of the bone in the BP-treated group. **(G)** Scanning electronic microscopy (SEM) analysis showed collapsed collagen fibers in the necrotic jaw bone of the BP-treated group and normal collagen of the control group at baseline. Transmission electron microscopy (TEM) revealed pyknosis of the nuclei (*upper panel*) and empty bone lacuna (*lower panel*). **(H)** Hematoxylin and eosin (H&E) staining of the minipig BRONJ model showed the presence of fibrosis and inflammatory infiltrate areas and necrotic bone (NB) areas with empty lacunae and fibrosis (scale bar = 50  $\mu\text{m}$ ). **(I)** Histological analysis of normal swine jawbones showed regular arrangement of the lamina and active osteocytes in lacunae (scale bar = 50  $\mu\text{m}$ ). **(J)** The area of fibrosis and inflammatory infiltrate over the tissue area were significantly higher in the jawbones of minipigs with BRONJ ( $***P < 0.001$ ). **(K, L)** Trichrome staining of BRONJ **(K)** and normal **(L)** swine jawbones showing necrotic bone and a lack of new bone (osteoid, red staining) in the jaws from minipigs with BRONJ (scale bar = 200  $\mu\text{m}$ ). **(M)** The area of osteoid over the tissue area was significantly decreased in the jawbones of minipigs with BRONJ ( $**P < 0.01$ ).



### Multilineage differentiation potential

BMMSCs were cultured in adipogenic differentiation and osteogenic differentiation media. Oil-red-O stain, alizarin red stain, and real-time (RT) PCR of *PPAR $\gamma$ 2* and alkaline phosphatase (*ALP*) were used to determine the BMMSC differentiation potential (see Supplementary Methods for details).

### Immunological changes in peripheral blood mononuclear cells

To investigate the immunological changes in the minipigs, we obtained blood from the precaval vein and performed

flow cytometric staining analysis using the immunological markers CD3, CD4 (Abcam), CD25 (AbD Serotec), and  $\gamma\delta T$  (VMRD) cells and Q-PCR detection of Foxp3 and interleukin (IL)-17 expression at 0, 4, 8, 16, and 24 weeks after BMMSC transfusion (see Supplementary Methods for details).

### RT-PCR for assessing gene expression

Samples were frozen and crushed into powder. Total mRNA was extracted and reverse transcribed. We obtained the gene sequences for *ALP*, tartrate-resistant acid phosphatase (*TRAP*), *IL-6*, and interferon- $\gamma$  (*IFN- $\gamma$* ) from GenBank. The cDNAs were amplified by PCR with the following

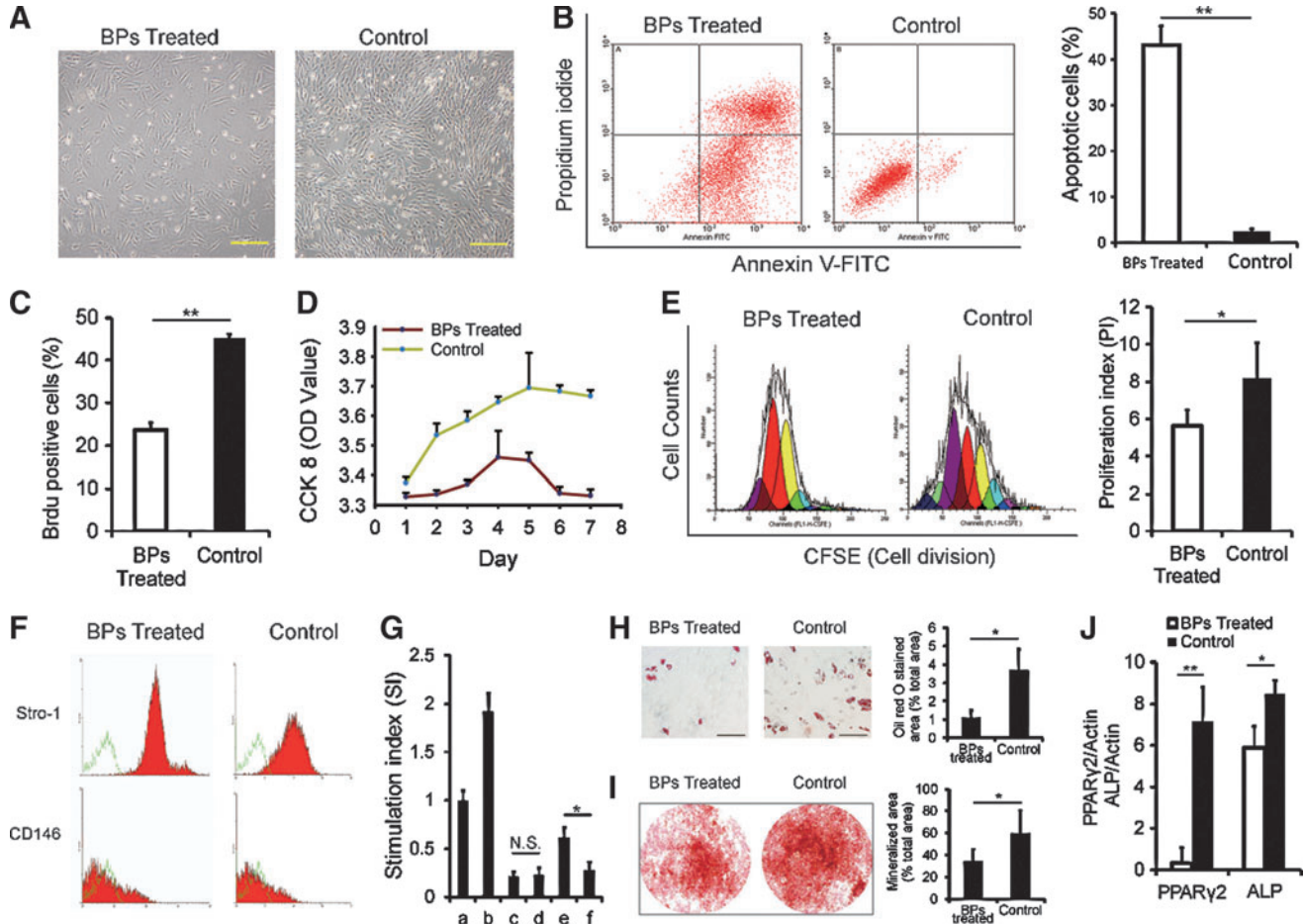


**FIG. 2.** Impairment of biological and immunological functions of BMMSCs in the BP-treated minipigs. (A) BMMSCs in the BP group could hardly adhere compared with controls 1 week after isolation (scale bar=2.0 mm). (B) Annexin V staining for apoptosis showed that ~43% of BMMSCs from the BRONJ group were positive for the early or late stages of apoptosis, but fewer apoptotic cells ( $4.14\% \pm 0.6\%$ ) were found in the untreated control group (\*\* $P < 0.01$ ). (C) Quantified BrdU-positive cells were significantly decreased in the BP-treated groups (\*\* $P < 0.01$ ). (D) CCK-8 tests showed a decreased proliferative ability of cells in the BP groups compared with the untreated group. (E) The carboxyfluorescein succinimidyl ester (CFSE) test indicated a declined proliferation index (\* $P < 0.05$ ) in the treatment group compared with the untreated control group. (F) There was no significant difference between the treatment and untreated control groups for both the Stro-1 and CD-146 markers (Stro-1:  $64.38\% \pm 1.19\%$  vs.  $64.46\% \pm 0.93\%$ ; CD-146:  $58.89\% \pm 0.42\%$  vs.  $55.17\% \pm 0.81\%$ , both  $P > 0.05$ ). (G) In mixed lymphocyte reaction, when tested with CCK-8, there was no difference in the stimulation index between the BP and control groups ( $0.19\% \pm 3.2\%$  vs.  $0.21\% \pm 4.3\%$ ,  $P > 0.05$ ), when mixed PBLs and BMMSCs, in the presence of phytohemagglutinin (PHA), the stimulation index increased in the BP groups ( $0.57\% \pm 9.6\%$  vs.  $0.22\% \pm 6.5\%$ , \* $P < 0.05$ ) (a: PBLs; b: PBLs+PHA; c: PBLs+BMMSCs of BP groups; d: PBLs+BMMSCs of control group; e: PBLs+PHA+BMMSCs of BP groups; f: PBLs+PHA+BMMSCs of control group). (H) The differentiation potential of BMMSCs stained with Oil red O or (I) alizarin red S (scale bar = 50  $\mu$ m) is shown; BMMSCs from BP-treated animals have significantly lower adipogenic differentiation and osteogenic differentiation potential (\*\* $P < 0.01$ ). (J) Q-PCR showed that *PPAR $\gamma$ 2* and alkaline phosphatase (*ALP*) were expressed. Adipose potential, as well as osteogenic potential, was significantly different between the treatment and untreated control groups (\*\* $P < 0.01$ ; \* $P < 0.05$ ).

thermocycler conditions: 95°C for 2 min, then 40 cycles of 95°C for 15 s, and 60°C for 1 min.

### Histological analysis and cell tracing in regenerated bone tissues

Tissue samples were taken from the necrotic area of three animals to perform histological analysis with hematoxylin and eosin (H&E) staining, trichrome staining, and TRAP staining. For osteoclast/osteoblast counting and fibrosis inflammatory area determination, the H&E-stained sections and TRAP-stained sections were photographed, and osteoclast/osteoblast count and fibrosis inflammatory area over tissue area were calculated per field at  $\times 200$  magnification by Image-Pro Plus version 6.0 software. For bone formation determination, trichrome-stained sections were photographed, and the red-stained area over tissue area was calculated per field at  $\times 200$  magnification by Image-Pro Plus version 6.0 software. Five sections for each animal were counted with an average of 10 fields/tissue by an experienced expert of histopathology under blinded fashion. Five fields per animal were analyzed for TRAP-stained sections. Samples collected from the cortical bone of BRONJ and control animals were examined under an S-520 scanning electron microscope and transmission electron microscope (Hitachi Company).

For cell tracing, BMMSCs from healthy male minipigs were transferred into female minipigs with BRONJ. Bone tissue was taken, and the sections were stained with an RBMY1 antibody 12 weeks later (see Supplementary Methods for details).

### Osteoid measurement

Bone samples were taken from the same extraction fields of the mandibles of minipigs. After trichrome staining, the sections were photographed, and the percentage of red-stained area (osteoid area) was calculated per field at  $\times 200$  magnification by Image-Pro Plus version 6.0 Software. Five entire sections for each animal were counted, with an average of 5 fields/section, by an experienced histopathology expert in a blinded fashion.

### BMMSC transplantation for treating BRONJ in minipigs

The animals with BRONJ were randomly divided into a BMMSC group treated with allogeneic BMMSCs ( $n=5$ ) from male minipigs and a group that was treated with physiological saline ( $n=3$ ). Minipigs in the untreated control group received no ZA treatment ( $n=3$ ) (see Supplementary Methods for details).

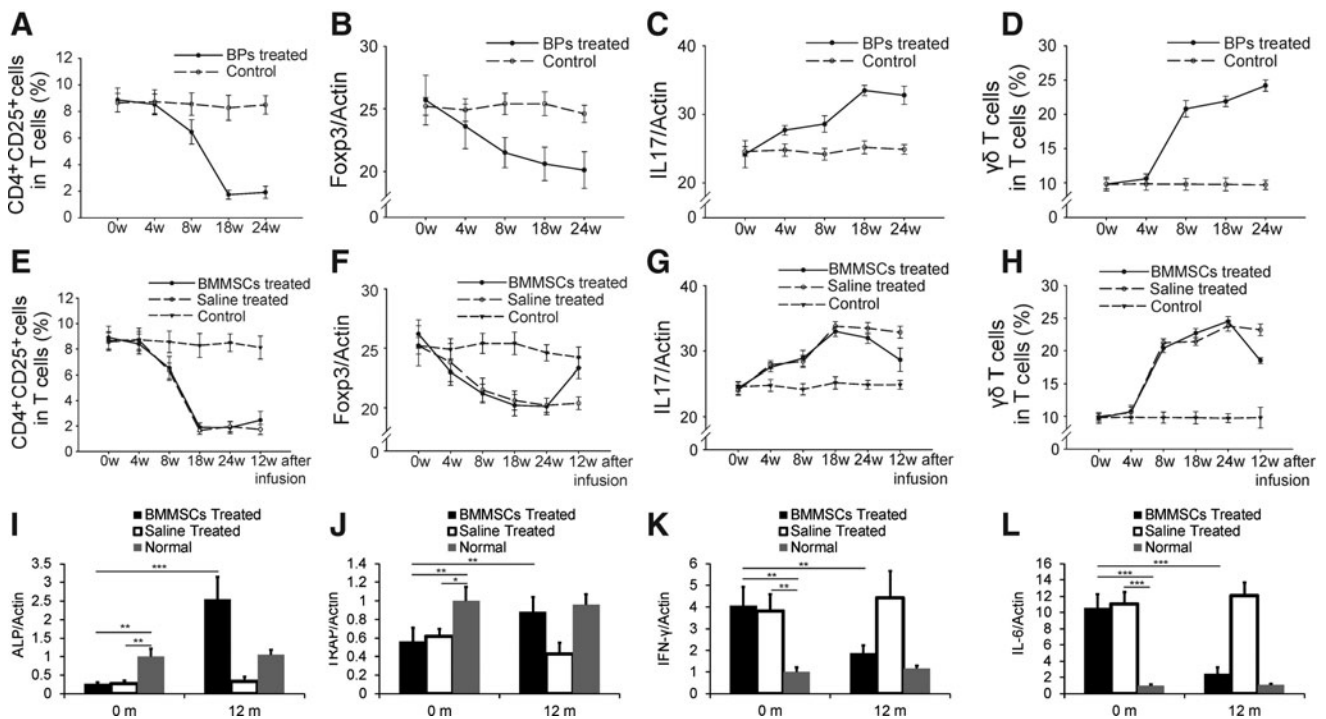


**FIG. 3.** Immunological changes in the BP-treated minipigs and bone remodeling and immunoregulation improvement after BMMSC infusion. (A)  $CD4^+CD25^+$  T-cells were significantly decreased in the peripheral blood from the BP-treated groups at 24 weeks after the BP treatment compared with the untreated control group ( $P < 0.05$ ). (B) BP treatment also resulted in slightly reduced  $Foxp3^+$  levels in the peripheral blood at 24 weeks after BP treatment ( $P = 0.05$ ). (C) interleukin (IL)-17 levels in the peripheral blood in the BP-treated groups were increased compared with the untreated control group at 24 weeks after BP treatment ( $P < 0.05$ ). (D) The levels of  $\gamma\delta$ T cells in the BP groups were significantly increased compared with the control group at 24 weeks after BP treatment ( $P < 0.05$ ). At 12 weeks after BMMSC transplantation, the level of  $CD4^+CD25^+$  T-cells recovered ( $P < 0.05$ ) (E); the level of  $Foxp3$  mRNA tended to increase in BRONJ minipigs ( $P < 0.05$ ) (F); and IL-17 levels were also reduced after treatment ( $P < 0.05$ ) (G). The level of  $\gamma\delta$ T cells in peripheral blood decreased in the BMMSC group ( $P < 0.05$ ) (H). The expression of  $ALP$  (I) and  $TRAP$  (J) increased 12 months after BMMSC treatment, whereas the levels of  $IFN-\gamma$  (K) and  $IL-6$  (L) decreased ( $*P < 0.05$ ;  $**P < 0.01$ ;  $***P < 0.001$ ). IFN, interferon; TRAP, tartrate-resistant acid phosphatase.

**FIG. 4.** Allogeneic BMMSC transplantation cured BRONJ in the minipig model. **(A)** The open alveolar socket with NB in the minipig model of BRONJ before BMMSC infusion (*black arrowhead*) (scale bar=1 cm). BRONJ minipigs that received BMMSC infusions showed healing with complete soft tissue 12 weeks and 12 months after infusion (scale bar=1 cm), whereas the exposure of NB in minipigs with BRONJ before saline infusion was still present with a wider exposure in the same minipigs with BRONJ (*black arrowhead*) 12 weeks and 12 months after saline infusion (scale bar=1 cm). **(B)** The CT image showing the necrotic right mandible of minipigs with BRONJ before BMMSC infusion and the disappearance of necrotic bone and healing of the BRONJ 12 weeks after BMMSC infusion (*yellow frame*) (scale bar=1 cm); more NB was found in the alveolar process (*yellow arrowhead*) and the lingual side of the right mandible 12 weeks after saline infusion (scale bar=1 cm). **(C)** Three-dimensional images of the CT scan also showed healing of the bony defects compared with the saline-treated group in the BMMSC-treated group 12 weeks after treatment.

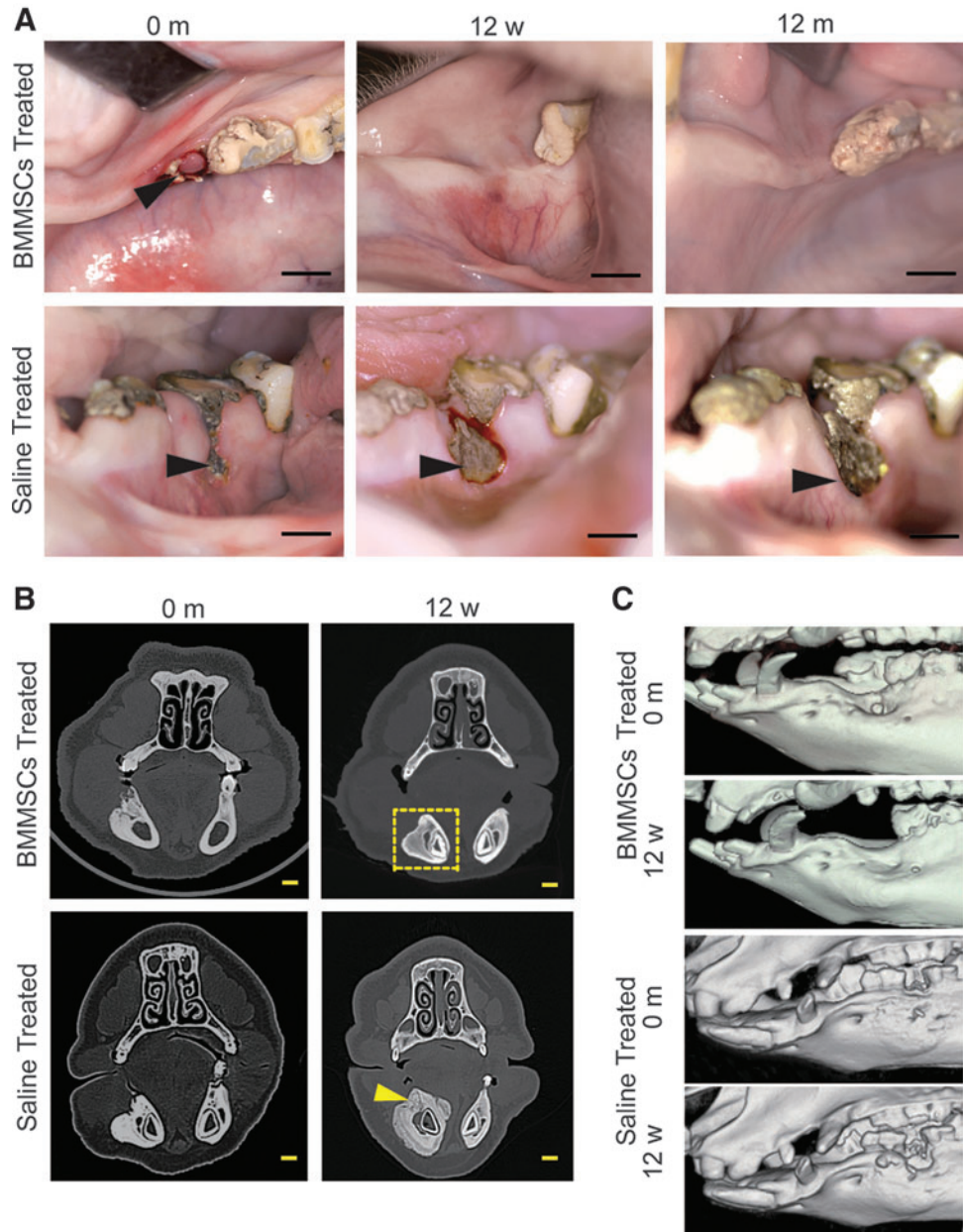
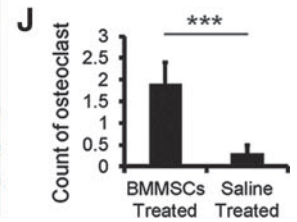
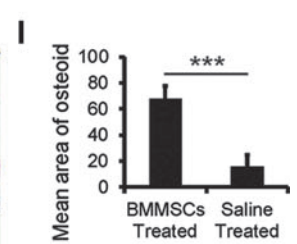
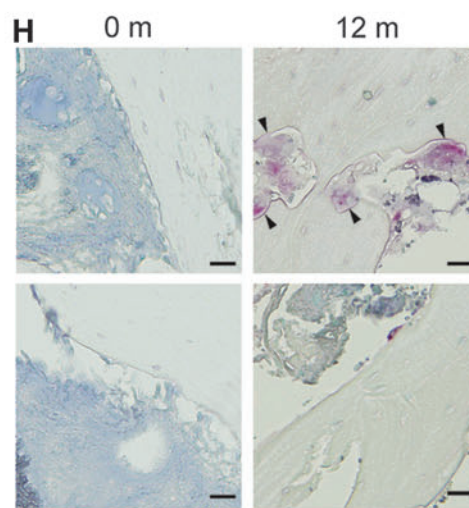
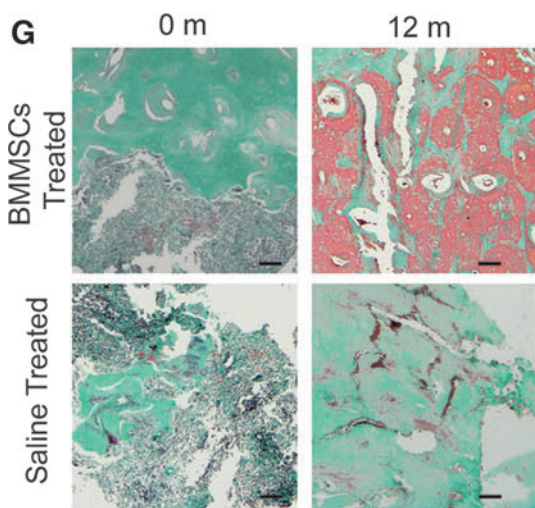
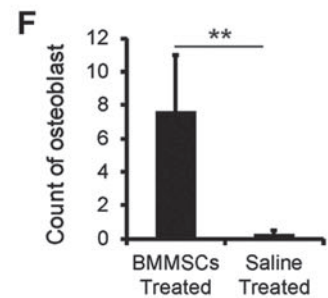
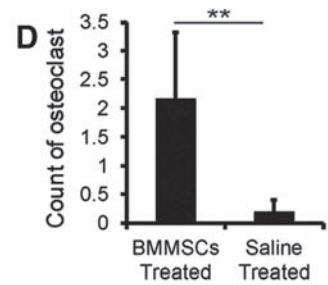
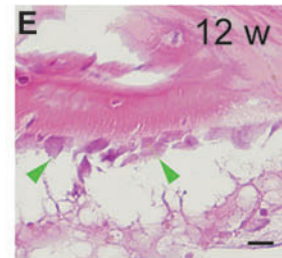
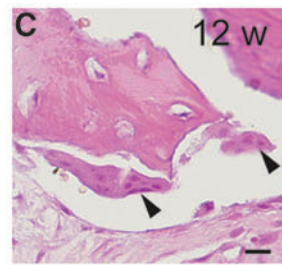
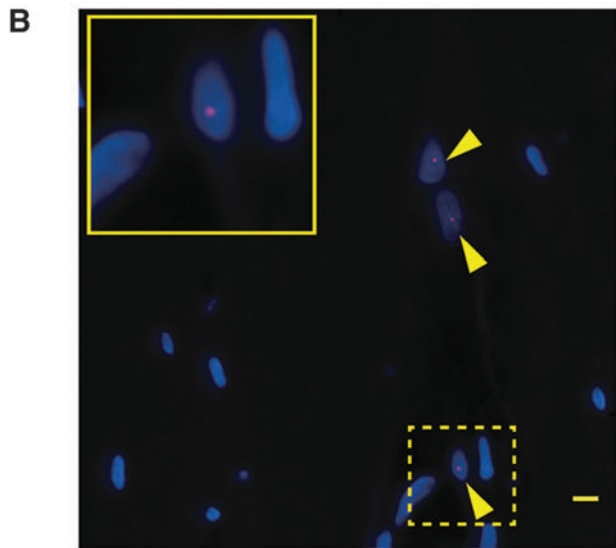
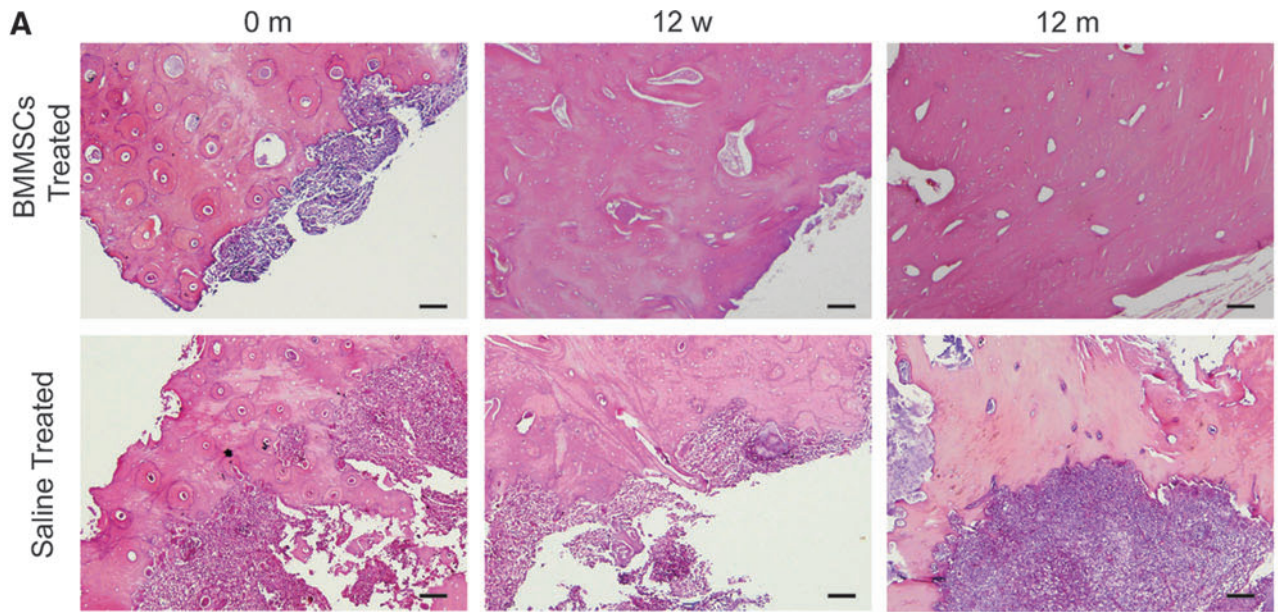


**FIG. 5.** Histological observation of bone reconstruction in the BMMSC-treated BRONJ minipig model. **(A)** H&E staining showed new bone formation in the NB area 12 weeks and 12 months after BMMSC infusion (scale bar=300  $\mu$ m), and NB was still present in minipigs with BRONJ treated with saline (scale bar=300  $\mu$ m). **(B)** Positive staining of Y-chromosomes (*red*) in regenerated bone of the BRONJ region (*yellow arrowhead*). **(C–F)** Bone remodeling of the mandible in minipigs after treatment with BMMSCs. Osteoclasts (*C*, *black arrowhead*) and osteoblasts (*E*, *green arrowhead*) were observed in H&E-stained sections 12 weeks after BMMSC infusions (bar=50  $\mu$ m). Means of osteoclast/field (*D*) and osteoblast/field (*F*) in H&E-stained sections were also significantly higher in the BMMSC-treated group  $**P < 0.01$ . **(G)** Trichrome staining revealed new bone formation (osteoid, red staining) in the collagen matrix (scale bar=300  $\mu$ m) of the group treated with BMMSCs 12 months postinfusion, whereas minipigs with BRONJ treated with saline showed no marked new bone formation (scale bar=300  $\mu$ m). **(H)** TRAP staining showed that the osteoclasts (*black arrowhead*) were observed in the group treated with BMMSCs 12 months postinfusion, whereas minipigs with BRONJ treated with saline showed few osteoclasts (bar=50  $\mu$ m). A significant increase in the osteoid area (*I*) and osteoclasts (*J*) over the tissue area in the group treated with BMMSCs compared with the group treated with saline ( $***P < 0.001$ ).



### Statistical analysis

Data were analyzed using one-way analysis of variance with pairwise comparisons using the Bonferroni method. *P* values <0.05 were considered significant.

## Results

### Minipig model of BRONJ induced by BP delivery

A clinically relevant BP delivery regimen was used to generate the large-animal model (Fig. 1A). Four weeks after tooth extraction, the clinical examination revealed incomplete mucosal healing in all BP-injected pigs (Fig. 1B). Eight weeks after tooth extraction, all BP-treated minipigs had exposed necrotic bone in the oral cavity (Fig. 1C) that persisted until stem cell treatment was administered. A CT scan showed destruction and enlargement of the cortical bone with both osteolysis and osteosclerosis in the necrotic jaw bone (Fig. 1D–F). Scanning electronic microscopy showed collapsed collagen fibers in the necrotic jaw bone (Fig. 1G, left). Transmission electron microscopy revealed pyknosis of the nuclei and empty bone lacuna (Fig. 1G, right). Histological analysis showed the presence of increased inflammatory infiltrates and necrotic bone areas with empty lacunae as well as fibrosis compared with normal bone (Fig. 1H–J). Measurement of osteoid from trichrome staining, which was sensitive for to mark the active bone formation, showed significant decreases in osteoid in minipigs with BRONJ compared with normal controls (Fig. 1K–M). These findings showed that a large-animal model of BRONJ was successfully established in the minipigs.

### Biological and immunological properties of BMMSCs were impaired in the BP-treated minipigs

BMMSCs from only two of the eight animals in the BP-treated group were successfully isolated and cultured because of the biological impairment (Fig. 2A); BP-treated BMMSCs also exhibited much more cell apoptosis than the control group (Fig. 2B). BrdU, CCK-8, and CFSE staining indicated a decreased proliferation of cells in the BP-treated groups (Fig. 2C–E). Flow cytometric analysis identified no significant differences in the surface markers of BMMSCs, including Stro-1 and CD146, between the BP-treated and control groups (Fig. 2F). In a mixed-lymphocyte reaction assay, the stimulation index in phytohemagglutinin-stimulated hPBLs was higher when cultured with BP-treated MSCs compared with the control MSCs (Fig. 2G). The adipose and osteogenic differentiation potential of BMMSCs was tested using Oil-red-O (Fig. 2H) and alizarin red S (Fig. 2I) staining, and *PPAR $\gamma$ 2* and *ALP* mRNA analysis (Fig. 2J). We found a significant difference in both adipose and osteogenic potential between the BP-treated and control groups.

### Regulatory T-cells were suppressed and IL-17 was increased in BP-treated minipig peripheral blood

Pigs treated with ZA showed a significant decrease in CD4<sup>+</sup>CD25<sup>+</sup> T-cells and *Foxp3* mRNA in the peripheral blood (Fig. 3A, B). In contrast, the levels of *IL-17* mRNA and  $\gamma\delta$ T cells in the peripheral blood of pigs in the treatment groups increased (Fig. 3C, D). The immunological changes

between the BP- and saline-treated groups began at week 4 and reached the highest level in week 24 (Fig. 3A–D).

### BMMSC-based therapy improved suppressed regulatory T-cells and elevated IL-17 levels in BRONJ minipigs

The effect of BMMSC on regulatory T-cells (Tregs) and IL-17 was found on 12 weeks after cell infusion (Fig. 3, E–H). After BMMSC transplantation, the level of CD4<sup>+</sup>CD25<sup>+</sup> T-cells and *Foxp3* expression increased in the BMMSC group (Fig. 3E, F). The IL-17 and  $\gamma\delta$ T cell levels were declined after BMMSC treatment (Fig. 3G, H). Moreover, the expression of *ALP* (Fig. 3I) and *TRAP* (Fig. 3J) increased 12 months after BMMSC treatment, whereas the level of *IFN- $\gamma$*  (Fig. 3K) and *IL-6* (Fig. 3L) decreased, indicating active bone remodeling and immunoregulation 12 months after BMMSC infusion.

### Allogeneic BMMSC transplantation cured BRONJ in minipigs

Twelve weeks after the BMMSC treatment, the open alveolar sockets of all five minipigs with BRONJ healed with complete soft tissue coverage, whereas the exposed necrotic bone with inflamed soft tissue still remained in the three saline-treated minipigs (Fig. 4A). CT examinations showed healing of the bony defects compared with the saline-treated group 12 weeks after BMMSCs infusion (Fig. 4B, C). Histological analysis showed new bone formation in previously necrotic areas (Fig. 5A) in BMMSC-treated minipigs with BRONJ 12 weeks and 12 months after infusion, and the appearance of osteoclasts (Fig. 5C, D) and osteoblasts (Fig. 5E, F), indicated bone remodeling 12 weeks after BMMSC treatment. Cell tracing showed positive Y-chromosome staining in the jaw bone of the BMMSC-treated animals 12 weeks after infusion, indicating that the transferred allogeneic BMMSCs mediated bone regeneration in the BRONJ lesion (Fig. 5B). A significant increase in the osteoid area over the tissue area and osteoclast count was observed (Fig. 5G–J), indicating marked new bone formation in the necrotic region. Taken together, BRONJ in minipigs was clinically cured by treatment with allogeneic BMMSC infusions.

## Discussion

BRONJ is defined as treatment with a BP, exposed necrotic bone for at least 8 weeks, and no history of radiation to jaws [3,4]. In the present study, we used a clinically relevant protocol of intravenous delivery of ZA and generated an animal model of BRONJ in minipigs successfully. Clinical and histological examinations and CT analysis showed jaw features, including sequestrum and radio-opaque alveolar bone. The exposed necrotic bone persisted until BMMSC treatment was administered, coinciding with the current diagnosis criteria of human BRONJ [3,4].

In daily activities, particularly during chewing, jaw bones are cyclically strained, leading to microdamage and bone reconstruction [10]. Although BPs do not inherently affect bone formation, they can affect bone formation indirectly through reductions in resorption. This may be a timing issue in that early on, bone formation was normal, but at the time of histological assessment, the osteoid was no longer being formed. Since jaw bones have frequent microdamage and



reconstruction, BP-related osteonecrosis happened there mostly. Previously, we developed a mouse model of BRONJ-like disease [6]; however, well-established large-animal models are needed for preclinical studies and will provide researchers with the opportunity to elucidate the mechanisms underlying BRONJ and to explore potential therapeutic approaches, particularly those that are difficult to implement in small-animal models such as rodents due to the small size of the orofacial region. Because of the high similarity between swine and humans in terms of histology and functions of the orofacial tissues [8,11,12], the miniature pig is increasingly used as a large-animal model for a variety of biomedical studies [13,14].

The findings from the present study showed that ZA treatment can suppress Treg levels in peripheral blood while increasing the levels of  $\gamma\delta$ T cells and IL-17 in peripheral blood. BPs can increase the level of IL-17 and  $\gamma\delta$ T cells and decrease the level of Tregs, suggesting that BPs can affect the function of cells in both the innate and acquired immunity pathways [15]. Macrophages could phagocytose apoptotic cells and secrete TGF- $\beta$ , which could induce Treg differentiation. However, osteoclasts, monocytes, and macrophages are the cells most likely to be affected by the administration of BPs. Additionally, it was reported that serum IL-6 increased on days 1 and 2 after ZA infusion [16]. Since IL-6 participates in driving Th17 differentiation with TGF- $\beta$ , more TGF- $\beta$  was consumed in Th17 differentiation. The BP-induced decrease in TGF- $\beta$  and increase in IL-6 may contribute to suppressed Treg levels in peripheral blood. Th17 cells are important in the pathogenesis of several inflammatory diseases such as multiple sclerosis and rheumatoid arthritis [17], whereas  $\gamma\delta$ T cells play a significant role in innate immunity against pathogens and also produce IL-17 [18]. Our data suggest that ZA treatment enhances the immune response in minipigs, which may be involved in the pathogenesis of BRONJ.

BMMSCs have the capacity to self-renew and differentiate into different cell lineages [19–21] and have unique immunomodulatory properties, both in vitro and in animal models and humans [22,23]. In the present study, we recognized a decreased proliferative capacity of BMMSCs after BP use, and ZA induced MSC apoptosis. Thus, an impaired BMMSC function may also contribute to the pathogenesis of BRONJ.

Previously, post-BP-treated autogenic bone marrow progenitor cells, including hematopoietic, mesenchymal, endothelial, and other progenitor cells, were used locally in jaw bone to treat BRONJ in humans [24]. However, we have showed in the present study that BMMSCs in BP-treated bone marrow were impaired. BMMSCs are capable of homing in to injured tissues after intravenous delivery [25] and are capable of anti-inflammatory effects [26]. The data from the present study based on a minipig model of BRONJ showed complete healing of the soft tissue as well as primary healing of the bony defects after infusion of BMMSCs. Since no specific treatments, including surgery for the necrotic bone, was delivered, we believed that the infused BMMSCs can migrate to local necrotic bone for vascular regeneration and bone reconstruction [9]. In the present study, we also found tracer cells in bone 12 weeks after infusion. After systemic infusion of BMMSCs, BP-induced increases in IL-17 and  $\gamma\delta$ T cells in the peripheral blood were markedly suppressed, whereas the decreased levels of Tregs observed in

the peripheral blood were partially restored. The restoration of impaired immunity by systemic infusion of BMMSCs may play an important role in curing BRONJ.

In summary, we successfully established a large-animal model of BRONJ in minipigs that more closely mimics the disease in humans and provides direct evidence of a link between BPs and osteonecrosis of the jaw. More importantly, we discovered that allogeneic BMMSC-based infusion provides a safe and effective therapeutic modality for treating BRONJ, which sheds light on potential clinical applications for treating BRONJ patients.

## Acknowledgments

This work was supported by the Beijing Municipal Committee for Science and Technology no. Z121100005212004, National Basic Research Program of China no. 2007CB947304 and no. 2010CB944801; Beijing Municipality no. PHR20090510, no. PXM 2009-014226-074691, and no. PXM2011-014226-07-000066; and a grant from NIDCR no. R01DE017449.

## Author Disclosure Statement

The authors declare that they have no competing interests.

## References

- Ruggiero SL, B Mehrotra, TJ Rosenberg and SL Engroff. (2004). Osteonecrosis of the jaws associated with the use of bisphosphonates: a review of 63 cases. *J Oral Maxillofac Surg* 62:527–534.
- Burr DB and MR Allen. (2009). Mandibular necrosis in beagle dogs treated with bisphosphonates. *Orthod Craniofac Res* 12:221–228.
- American Association of Oral and Maxillofacial Surgeons. (2007). American Association of Oral and Maxillofacial Surgeons position paper on bisphosphonate-related osteonecrosis of the jaws. *J Oral Maxillofac Surg* 65:369–376.
- Ruggiero SL, TB Dodson, LA Assael, R Landesberg, RE Marx and B Mehrotra. (2009). American Association of Oral and Maxillofacial Surgeons position paper on bisphosphonate-related osteonecrosis of the jaws. *J Oral Maxillofac Surg* 67:2–12.
- Allen MR and DB Burr (2009). The pathogenesis of bisphosphonate-related osteonecrosis of the jaw: so many hypotheses, so few data. *J Oral Maxillofac Surg* 67:61–70.
- Kikuri T, I Kim, T Yamaza, K Akiyama, Q Zhang, Y Li, C Chen, W Chen, S Wang, AD Le and S Shi. (2010). Cell-based immunotherapy with mesenchymal stem cells cures bisphosphonate-related osteonecrosis of the jaw-like disease in mice. *J Bone Miner Res* 25:1668–1679.
- Migliorati CA, JB Epstein, E Abt and JR Berenson. (2011). Osteonecrosis of the jaw and bisphosphonates in cancer: a narrative review. *Nat Rev Endocrinol* 7:34–42.
- Wang S, Y Liu, D Fang and S Shi. (2007). The miniature pig: a useful large animal model for dental and orofacial research. *Oral Dis* 13:530–537.
- Xu J, Z Zheng, D Fang, R Gao, Y Liu, Z Fan, C Zhang, S Shi and S Wang. (2012). Mesenchymal stromal cell-based treatment of jaw osteoradionecrosis in swine. *Cell Transplantation* 21: 1679–1686.
- Eriksen, EF. (2010). Cellular mechanisms of bone remodeling. *Rev Endocr Metab Disord* 11:219–227.

11. Liu Y, Y Zheng, G Ding, D Fang, C Zhang, PM Bartold, S Gronthos, S Shi and S Wang. (2008). Periodontal ligament stem cell-mediated treatment for periodontitis in miniature swine. *Stem Cells* 26:1065–1073.
12. Xu J, X Yan, R Gao, L Mao, AP Cotrim, C Zheng, C Zhang, BJ Baum and S Wang. (2010). Effect of irradiation on microvascular endothelial cells of parotid glands in the miniature pig. *Int J Radiat Oncol Biol Phys* 78:897–903.
13. Gao R, X Yan, C Zheng, CM Goldsmith, S Afione, B Hai, J Xu, J Zhou, C Zhang, JA Chiorini, BJ Baum and S Wang. (2011). AAV2-mediated transfer of the human aquaporin-1 cDNA restores fluid secretion from irradiated miniature pig parotid glands. *Gene Ther* 18:38–42.
14. Shan Z, J Li, C Zheng, X Liu, Z Fan, C Zhang, CM Goldsmith, RB Wellner, BJ Baum and S Wang. (2005). Increased fluid secretion after adenoviral-mediated transfer of the human aquaporin-1 cDNA to irradiated miniature pig parotid glands. *Mol Ther* 11:444–451.
15. Chen YJ, KS Chao, YC Yang, ML Hsu, CP Lin and YY Chen. (2009). Zoledronic acid, an aminobisphosphonate, modulates differentiation and maturation of human dendritic cells. *Immunopharmacol Immunotoxicol* 31:499–508.
16. Karga H, I Giagourta, G Papaioannou, P Katsichti, A Pardalakis, G Kassi, A Zagoreou, M Triantaphyllopoulou and C Zerva. (2011). Transient changes in thyroid functions tests after zoledronic acid infusion. *Endocr J* 58:969–977.
17. Lubberts E. (2010). Th17 cytokines and arthritis. *Semin Immunopathol* 32:43–53.
18. Casetti R and A Martino. (2008). The plasticity of gamma delta T cells: innate immunity, antigen presentation and new immunotherapy. *Cell Mol Immunol* 5:161–170.
19. Prockop DJ. (1997). Marrow stromal cells as stem cells for nonhematopoietic tissues. *Science* 276:71–74.
20. Phinney DG and DJ Prockop. (2007). Concise review: mesenchymal stem/multipotent stromal cells: the state of transdifferentiation and modes of tissue repair—current views. *Stem Cells* 25:2896–2902.
21. Bernardo ME, F Locatelli and WE Fibbe. (2009). Mesenchymal stromal cells. *Ann N Y Acad Sci* 1176:101–117.
22. Nauta AJ and WE Fibbe. (2007). Immunomodulatory properties of mesenchymal stromal cells. *Blood* 110:3499–3506.
23. Wolf D and AM Wolf. (2008). Mesenchymal stem cells as cellular immunosuppressants. *Lancet* 371:1553–1554.
24. Cella L, A Oppici, M Arbasi, M Moretto, M Piepoli, D Valisa, A Zangrandi, C Di Nunzio and L Cavanna. (2011). Autologous bone marrow stem cell intralesional transplantation repairing bisphosphonate related osteonecrosis of the jaw. *Head Face Med* 7:16.
25. Chamberlain G, J Fox, B Ashton and J Middleton. (2007). Concise review: mesenchymal stem cells: their phenotype, differentiation capacity, immunological features, and potential for homing. *Stem Cells* 25:2739–2749.
26. Bonfield TL, M Koloze, DP Lennon, B Zuchowski, SE Yang and AI Caplan. (2010). Human mesenchymal stem cells suppress chronic airway inflammation in the murine ovalbumin asthma model. *Am J Physiol Lung Cell Mol Physiol* 299:L760–L770.

Address correspondence to:

Songlin Wang  
Capital Medical University School of Stomatology  
Tian Tan Xi Li No. 4  
Beijing 100050  
China

E-mail: slwang@ccmu.edu.cn

Songtao Shi  
Center for Craniofacial Molecular Biology  
Herman Ostrow School of Dentistry  
University of Southern California  
Los Angeles, CA 90089

E-mail: songtaos@usc.edu

Received for publication November 4, 2012

Accepted after revision March 1, 2013

Prepublished on Liebert Instant Online March 6, 2013